First-principles calculations of the instability leading to the Invar effect

P. Entel and E. Hoffmann
Theoretische Tieftemperaturphysik and SFB 166, Universität-GH-Duisburg, W-4100 Duisburg 1, Germany

P. Mohn and K. Schwarz
Technische Universität Wien, A-1060 Wien, Austria

V. L. Moruzzi
IBM Thomas J. Watson Research Center, Yorktown Heights, New York 10958
(Received 18 September 1992)

An attempt is made to show the close connection between martensitic transformations, the Invar effect, magnetovolume instabilities, and associated low-moment–high-moment (LM-HM) transitions. For that purpose we study the volume dependence of electron occupation and magnetization of e_g and t_{2g} states in ordered Fe_3Ni. We show that in this compound the instability against small tetragonal distortions, the Invar behavior, and the LM $\rightleftharpoons$ HM transitions are a consequence of the delicate balance of charge distribution and magnetic order from d orbitals having different bonding character. Our calculation is a generalization of the cluster calculation of Kaspar and Salahub who have speculated that the Invar effect is a consequence of thermal excitations of electrons from the antibonding majority-spin level to close-lying nonbonding minority-spin orbitals at the Fermi energy E_F. Our fixed-spin-moment (FSM) calculation confirms the presence of these orbitals close to E_F in Fe_3Ni. In addition we have extended the FSM calculations to finite temperatures with the help of a semimicroscopic spin-fluctuation theory, which allows the study of the temperature evolution of the HM and LM states of Fe_3Ni. We find that the states merge with increasing temperature.

I. INTRODUCTION

Certain transition-metal alloys like Invar, $Fe_{0.64}Ni_{0.36}$,[1] exhibit unusual thermal properties typified by an anomalously low thermal expansion near room temperature. Currently these properties are assumed to be a consequence of the existence of a magnetovolume instability within the range of thermal excitations (for a recent survey see Ref. 2). Although the general features of the Invar effect can be qualitatively understood in terms of this instability, a detailed microscopic theory of Invar is still missing.

An attempt to introduce a detailed picture of the Invar effect was undertaken by Weiss.[3] He introduced two states labeled γ_1 and γ_2, where the first one is associated with large volumes and high magnetic moments (HM) and the latter one with small volumes and low magnetic moments (LM).[59] The Invar effect is then driven by a thermal depopulation of γ_1 and subsequent population of γ_2. This so-called two-states model was successfully applied to explain experimental findings. In spite of its success, this model is a purely phenomenological statistical model and the actual existence (i.e., the simultaneous presence) of the two states has never been verified experimentally.

This fact led other authors to introduce Invar models where the existence of separated LM and HM states is no longer a necessary prerequisite. Kakehashi (for recent reviews and further references therein see Refs. 4 and 5) assumes that the Invar effect is a consequence of a gradual transition from strong to weak magnetism due to thermal excitations. In the actual calculation, Kakehashi used the single-site spin-fluctuation theory. In order to do the functional integration he had to assume a very simple model density of states to account for the actual electronic structure of Fe_3Ni (Ref. 6). Investigations along similar lines were undertaken by Hasegawa[7,8] who found that with increasing iron content, the ratio of the root-mean-square value of local magnetic moments at T_c to the ground-state moment, becomes small in the Invar region. This, in turn, leads to a large spontaneous volume magnetostriction ω_s in the Invar alloy.

By going beyond the single-site theory Kakehashi showed that local environment effects on the local moments are very important for the magnetization versus concentration curve in Fe-Ni alloys. Although the results describe the experimental trends quite well, drastic approximations were made to overcome the mathematical difficulties in solving the finite temperature band theory including the effect of spin fluctuations.

Williams *et al.*[9] used band-structure calculations to give the phenomenological Weiss model a quantum-mechanical basis and to provide an itinerant electron interpretation. They used an ordered Fe_3Ni structure to simulate the Invar alloy and found that the ferromagnetic ground state has its equilibrium at a larger volume than the nonmagnetic state which lies slightly higher in energy. Recent high-precision calculations[10] verified the existence of an additional low-moment state leading to a magnetovolume instability. On the basis of these results

the Invar effect is explained by the specific temperature evolution of the LM and HM states which are assumed to merge at high temperatures. However, the nature of the mixing of these states remains unclear.

In spite of its simplicity, the model has proven to be very successful. Moruzzi[11] has shown that the gradual transition from the high-volume (HM) to the low-volume (LM) state with increasing temperature can be accounted for by combining total-energy-band calculations with the Debye-Grüneisen theory. In his formulation the temperature evolution of the free energy is governed by volume-dependent quantities, the rigid-lattice total energy $E(V)$ and the volume dependence of the Debye temperature $\Theta=\Theta_0(V_0/V)^\gamma$, where V is the volume and V_0 is the rigid-lattice equilibrium volume. By choosing a different set of thermal parameters (V_0, Θ_0, and γ) for the HM and LM branches of ordered Fe_3Ni, Moruzzi observed that Invar behavior requires that the HM solution defines the *ground state* at low temperatures, while the LM solution leads to the *ground state* at high temperatures. This theory qualitatively explains the anomalous temperature dependence of the thermal expansion, bulk modulus, magnetization, high-field susceptibility, and the different pressure dependencies of the lattice constant at different temperatures of Invar.

A different microscopic investigation was undertaken by Johnson *et al.*[12–14] They used a self-consistent KKR-CPA study of the Fe-Ni system for different volumes and investigated the competition between bonding and magnetism. More recently they used a mean-field statistical mechanics approach at finite temperatures which uses the accurate KKR-CPA energy for the configurationally averaged energy as input. With increasing Fe content, the theory predicts a crossover in the Invar region from the HM state to a state of magnetic disorder and then to a nonmagnetic state. This should be the underlying mechanism that produces the Invar phenomena. In contrast to Moruzzi's picture, here, one has more than two competing states.

The possibility of stabilizing competing states with different magnetic moments and different volumes but equal total energy is very intriguing. In this context, recent computer simulations in which itinerant magnetism of fictitious amorphous Fe and realistic $Fe_{1-x}Zr_x$ alloys were studied by Krey *et al.*[15] In these simulations, 54 atoms with periodic boundary conditions were used. The position of the atoms was relaxed to metastable equilibrium in Lennard-Jones potentials, while the electronic contribution was described by a Hartree-Fock decomposed multiband-Hubbard model together with a Koster-Slater parametrization.[16,17] These authors observed that stable or metastable solutions with different average magnetic moments have nearly equal total energy and density of states, but can be stabilized by changing the magnetic history of the sample, which could be effected in the simulation by changing the value of the external magnetic field. The authors also observed HM$\rightleftharpoons$LM transitions at specific volumes.

In a subsequent paper this method was applied to disordered iron-nickel Invar alloys with particular emphasis on the Invar region around 65% Fe.[18] It is remarkable that these model calculations reproduce the experimental magnetization curve in the whole concentration range. In addition they found that the drastic change in the Invar region comes from the dependence of the Fe moments on the concentration and environment. Since this calculation was carried out for $T=0$ only, information about the Invar effect was derived from the volume dependence of the magnetization per atom. Magnetovolume effects were solely driven by the Fe moments, since the Ni moments remain constant around the Invar composition (65% Fe). The relatively smooth increase of the magnetization with volume suggests that in the actual disordered Invar alloy there are not only two Fe states with different moments and different lattice constants as proposed by the Weiss model or by the binding surface of Fe_3Ni, but a continuum of states. These observations agree with the findings of Kakehashi and Johnson *et al.* that more than two dominating states are important. Moreover, the older hypothesis which attributes the Invar effect to an antiferromagnetic interaction between localized Fe spins[19–21] seems to be incorrect and thus a theory (at least at low temperatures) should be based on band-theoretical calculations rather than on Heisenberg-like models.

Moreover, we would like to point out that despite elaborate band calculations it has never become clear why the stabilization of competing magnetic states should happen at the magic occupation numbers of 8.6 electrons per atom in ferromagnetic and at 7.7 electrons/atom in antiferromagnetic Invar alloys.[22–24] It remained unclear to which extent the magnetovolume instabilities, the Invar behavior, and martensitic transformations are interrelated. This connection between different physical properties in a series of fcc $3d$ alloys and the electron concentration per atom was qualitatively explained by Wassermann[22,23] on the basis of recent band-structure calculations.[24–27] He showed that the calculated energy difference[24,25,27] between LM and HM states, $\Delta E=E_{\mathrm{LM}}-E_{\mathrm{HM}}$, as a function of the electron concentration, e/atom, becomes very small at the threshold values 7.7 and 8.6. Small changes in the electron concentration around these thresholds lead to anomalous behavior of physical quantities such as the spontaneous volume magnetostriction at zero temperature ω_s, the thermal expansion coefficient at room temperature α_{RT}, the Debye temperature Θ_D, and the electronic specific-heat coefficient γ. Note that these anomalously large variations of physical quantities in the Invar region with small changes of e/atom or of ΔE bring us back to the phenomenological Weiss model. Wassermann discussed the similarity between calculated ΔE as a function of e/atom and the curve representing the Weiss model. However, we repeat that the occurrence of two competing magnetic states (with different volumes) at finite temperatures has not yet been found. What has been observed by Mössbauer measurements on $Fe_{68.5}Ni_{31.5}$ and $Fe_{72}Ni_{28}$ is a gradual transition from the HM to the LM state at low temperatures under high enough pressure.[28]

A completely different explanation of the origin of the Invar effect was given by Kaspar and Salahub,[29] who performed calculations on small clusters (Fe_{13}, $Fe_{12}Ni$, and

Ni_{13}). They used the energy levels together with the rigid-band model to explain the Invar effect and argued that the anomaly is due to a special position of the Fermi level in the ferromagnetic electronic structure of the Fe-Ni alloy, which shows a rather peculiar situation at the Invar Fermi level. They found that for a narrow range of Ni concentration, strongly antibonding majority-spin orbitals and nonbonding minority-spin orbitals lie close in energy. They attribute the Invar effect to thermal excitations of electrons from the antibonding majority spin just below E_F to nonbonding minority-spin states just above E_F resulting in a contraction of the bonds which can counteract the vibrational lattice expansion.

Recently, these conclusions of Kaspar *et al.* were criticized by Podgorny,[30] who argues that their energy-level diagrams do not resemble the actual energy bands of either Fe or Ni. Podgorny investigated the electronic structure of the ordered structures Fe_3Ni, Fe_5Ni_3, and Fe_2Ni_2, where the second is close to the $Fe_{65}Ni_{35}$ composition. He finds a crossover from strong to weak ferromagnetism between Fe_2Ni_2 and Fe_3Ni at the Invar composition Fe_5Ni_3, which is just at the borderline. He ascribes the Invar effect in accordance with Moruzzi to nearly degenerate HM and LM states.

Apart from first-principle band structure or cluster calculations, there exists a different approach based on a Ginzburg-Landau (GL) formulation of magnetovolume effects which has proven to be quite successful.[31–35] A magnetovolume term is included in the GL expression of the free energy of a ferromagnet $[\mathcal{H}=\frac{1}{2}B\omega^2+a(\omega_c-\omega)m^2+bm^4+\cdots]$, giving rise to a spontaneous volume magnetostriction at zero temperature, $\omega_m=(V-V_0)/V_0=\kappa a m_0^2$, where $\kappa=1/B$ is the compressibility, a a coupling constant, and m_0 the uniform magnetization. Moriya and Usami improved this result by allowing for longitudinal and transverse spin fluctuations which were integrated out following the mode-mode coupling theory of Murata and Doniach.[36] With spin fluctuations the change in volume between $T=0$ and $T=T_c$ is now $\frac{2}{5}\kappa a m_0^2$ instead of $\kappa a m_0^2$.

Recently Takahashi[37] confirmed the results of Moriya *et al.* using a different approach in which the local spin-fluctuation amplitude is assumed to be nearly constant, as in weakly ferromagnetic metals. He found it essential to retain a q-dependent magnetovolume coupling constant in order to obtain a large magnetovolume effect. He finds that, in general, the magnetostriction is not proportional to m^2, but to the reciprocal susceptibility.

In spite of its simplicity this GL formulation contains interesting features and becomes a first-principle scheme when the GL coefficients are determined by means of band-structure calculations using the fixed-spin-moment (FSM) method,[38,39] which provide zero-temperature binding surfaces as a function of magnetic moment and volume.[40–49] This functional, with the help of spin-fluctuation theory, allows a description of HM and LM states and their thermal evolution, and show that the LM and the HM states can merge together at the Curie temperature, similar to what happens in the Grüneisen formulation.

This short survey of a few selected Invar theories shows that there are different and also contradictory theories of the Invar effect.

The aim of this paper is to deepen our theoretical understanding of Invar and martensitic systems and to try to resolve the contradictions. In order to do this we have concentrated on one particular system, namely Fe_3Ni, and have performed detailed fixed-spin-moment band-structure calculations.

One particular aim was to check whether the explanation of the Invar effect as given by Salahub *et al.* on the basis of cluster calculations holds also for the case of a stoichiometric, itinerant magnetic system. This is done in Secs. II and III. In Sec. II an e_g, t_{2g} description of the magnetovolume effects and the magnetovolume instability in Fe_3Ni is presented. In Sec. III a detailed discussion of band structures and densities of states (DOS) is given. We confirm the findings of Kaspar and Salahub, since we find antibonding majority- and nonbonding minority-spin states near the Fermi energy. However, in contrast to Salahub *et al.*, we associate the Invar effect with a pinning of the Fermi energy in a pseudogap which opens at the Fermi surface due to symmetry breaking at finite temperatures by strong coupling of electrons to longitudinal and shear modes. At zero temperature, we mimic this dynamic symmetry breaking by a frozen phonon calculation (i.e., by allowing for tetragonal distortions). This distortion actually leads to such a pseudogap. We consider this pinning and the resulting stabilization of small distortions as a possible explanation for the formation of premartensite in Invar.

Furthermore, we show in Sec. III that ordered Fe_3Ni is unstable with respect to a martensitic transformation from the high-temperature face-centered structure to the low-temperature body-centered structure. We argue that this instability is not only a consequence of large magnetovolume coupling, but it seems to be related to coherent electron scattering connected with Fermi-surface nesting. The implication of this transformation for the Invar effect will be discussed in some detail. In order to demonstrate how close in concentration Invar and martensite are, we show in Fig. 1 the phase diagram of the Fe-Ni system.[2,50] Because of this closeness, we believe that calculations for hypothetical fcc Fe_3Ni can yield information about the underlying microscopic mechanism which gives rise to the Invar effect.

The involvement of lattice degrees of freedom in Invar leads to an unusual temperature behavior of the longitudinal elastic constant C_L and the elastic shear constants C_{44} and C' for the Invar alloy $Fe_{65}Ni_{35}$.[51] All three elastic constants show pronounced softening over the temperature range for which the thermal-expansion coefficient is practically zero. Therefore, Invar effects and effects associated with the onset of a structural transformation in the Fe-Ni system must be related since $Fe_{65}Ni_{35}$ is close to this transition. It is further remarkable that the difference between the shear moduli of the hypothetical paramagnetic state and the magnetic state, ΔC_{44} and $\Delta C'$, scale with m^2, while the longitudinal

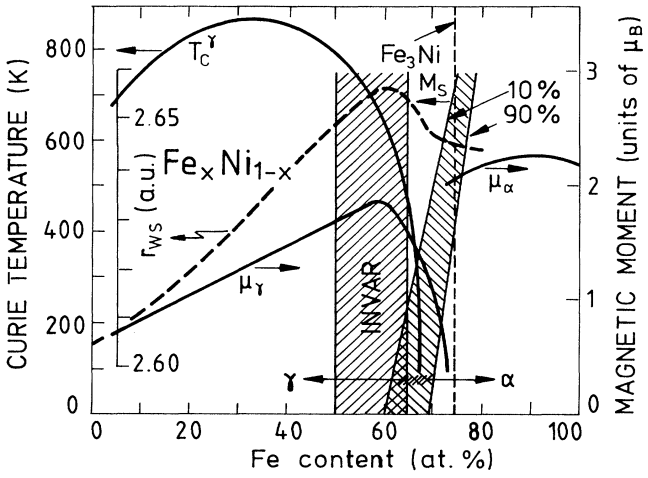

FIG. 1. Magnetic and structural phase diagram of Fe_xNi_{1-x} (Ref. 2). Curie temperatures in the γ phase and the magnetic moment in the α and γ phase are given as function of the Fe concentration. In addition, the martensitic transition temperatures corresponding to 10 and 90% martensitic transformation are shown. Note the closeness of the HM-Invar region and the region of structural $\gamma \rightarrow \alpha$ transformation. Also shown is the Wigner-Seitz radius at $T=290$ K. It displays a maximum in the Invar region where the magnetization is maximal also.

modulus (which is associated with the volume change) does not obey a power law behavior, and that the softening starts far above the Curie temperature. As will be discussed in Sec. III, we believe that the Invar effect and the formation of martensite in Fe-Ni are just two different aspects of the system being close to a magnetovolume instability.

In Sec. IV we apply the FSM-GL theory to Fe_3Ni. In addition we discuss how this theory can be improved with the help of a many-body Hamiltonian which contains the essential ingredients of our FSM calculations. This leads to an order-parameter concept for Invar which is based on the mixing of antibonding majority- and nonbonding minority-spin states close to E_F.

Section V contains a summary of the most important results.

II. AN e_g, t_{2g} DESCRIPTION OF THE MAGNETOVOLUME INSTABILITY IN Fe_3Ni

It is well known from the band theory of transition metals that the exchange splitting of the d bands which leads to magnetism results in a transfer of charge from minority-spin to majority-spin states. This charge transfer usually occurs among antibonding orbitals near the top of the d bands and leads to an expansion of the volume and a reduction of the kinetic energy associated with the occupied s and p states (which, in turn, leads to a softening of the system as implied by the reduction of the bulk modulus).[52] With increasing temperature, the magnetization as well as the magnetic contribution to the lattice expansion decrease. This means that in *ideal* Invar alloys the decrease of the magnetic contribution to the lattice expansion would be exactly compensated by the usual thermal expansion of the lattice with increasing T. The question is, how is such an exact cancellation possible?

In this and the following section we show that the charge transfer among antibonding and nonbonding bands of different spin symmetry close to the Fermi energy E_F is different in Invar systems as compared to other itinerant magnets like bcc Fe and that this is of crucial importance for an understanding of Invar properties. First, FSM band calculations of ordered fcc Fe_3Ni show zero-field results which consist of LM solutions at small volumes and HM solutions at large volumes. The two types of solutions require the zero-field total energy $E(V)$ to be represented as two separate but crossing curves which terminate near the crossing point. This result implies a first-order magnetovolume transition from the LM to the HM state. At zero temperature, the ground state of Fe_3Ni corresponds to the HM high volume branch. However, the minimum of the LM low volume branch occurs at about 1 mRy above the HM branch, well within range of thermal excitations. These features are shown in the zero-field energy versus volume curves in Fig. 2(a). The volume dependence of the electronic charge, decomposed into e_g and t_{2g} contributions, is also shown in Fig. 2(a). As can be seen, the charge associated with e_g states decreases while the charge associated with t_{2g} states increases with increasing volume. At the critical volume marking the transition from the LM to the HM state, we note a discontinuity in the charges. That is, there is an abrupt transfer of charge from e_g to t_{2g} states at the magnetovolume instability. Note that this $e_g \rightarrow t_{2g}$ charge transfer, (i.e., charge transfer from $dd\pi$ bonds into $dd\sigma$ bonds) is necessary to stabilize the high moment and the large volume of the fcc lattice. Our investigations show that there is much less charge transfer among orbitals in bcc Fe when the lattice is expanded. Thus, Invar systems can be characterized by an anomalously large $e_g \rightarrow t_{2g}$ charge transfer on the HM side.

In Fig. 2(b) we show the calculated magnetic moments associated with iron and nickel e_g and t_{2g} states as a function of volume. The magnetovolume instability is manifested by the discontinuity in the moments. At the volume corresponding to the instability, the system can exhibit either HM or LM behavior with no change in energy. We note that although Fig. 2(a) implies an abrupt transfer of charge from e_g to t_{2g} states, Fig. 2(b) shows that on the LM side, LM iron moments are mostly of t_{2g} character while the HM iron moments are mostly of e_g character for the transition volume. On the other hand, the relatively large magnetic moments of t_{2g} charges on the HM side means that the HM high-volume state is stabilized by a substantial amount of covalent magnetic moments. For larger r_{WS} values, the iron t_{2g} moment again dominates. Second, as a function of volume, the majority-spin and minority-spin e_g and t_{2g} states associated with iron and nickel shift in energy. In Fig. 2(c) we show the energy relative to E_F of e_g and t_{2g} eigenvalues at the X point of the Brillouin zone and for energies close to the Fermi energy. We note the splitting of the states at the onset of the LM solutions. We also observe that

for the ground state of Fe_3Ni at $r_{WS}=2.605$ a.u. and in the vicinity of E_F, states of different bonding character and different spin symmetry cross. Slightly below E_F we find an occupied majority-spin X_3 state of mainly t_{2g}^* antibonding (AB) character and right at E_F the minority-spin X_4' state of mainly e_g^* AB character. In addition we have slightly above E_F, the unoccupied minority-spin X_5 state of mainly t_{2g} nonbonding (NB) character. The aim of this plot is to show that this specific level crossing, which corresponds to the level crossing found by Kaspar and Salahub in their cluster calculation, actually occurs only in the HM state for volumes close to the ground-state volume. It does not occur in the LM state or at the magnetovolume instability. We have checked other sym-

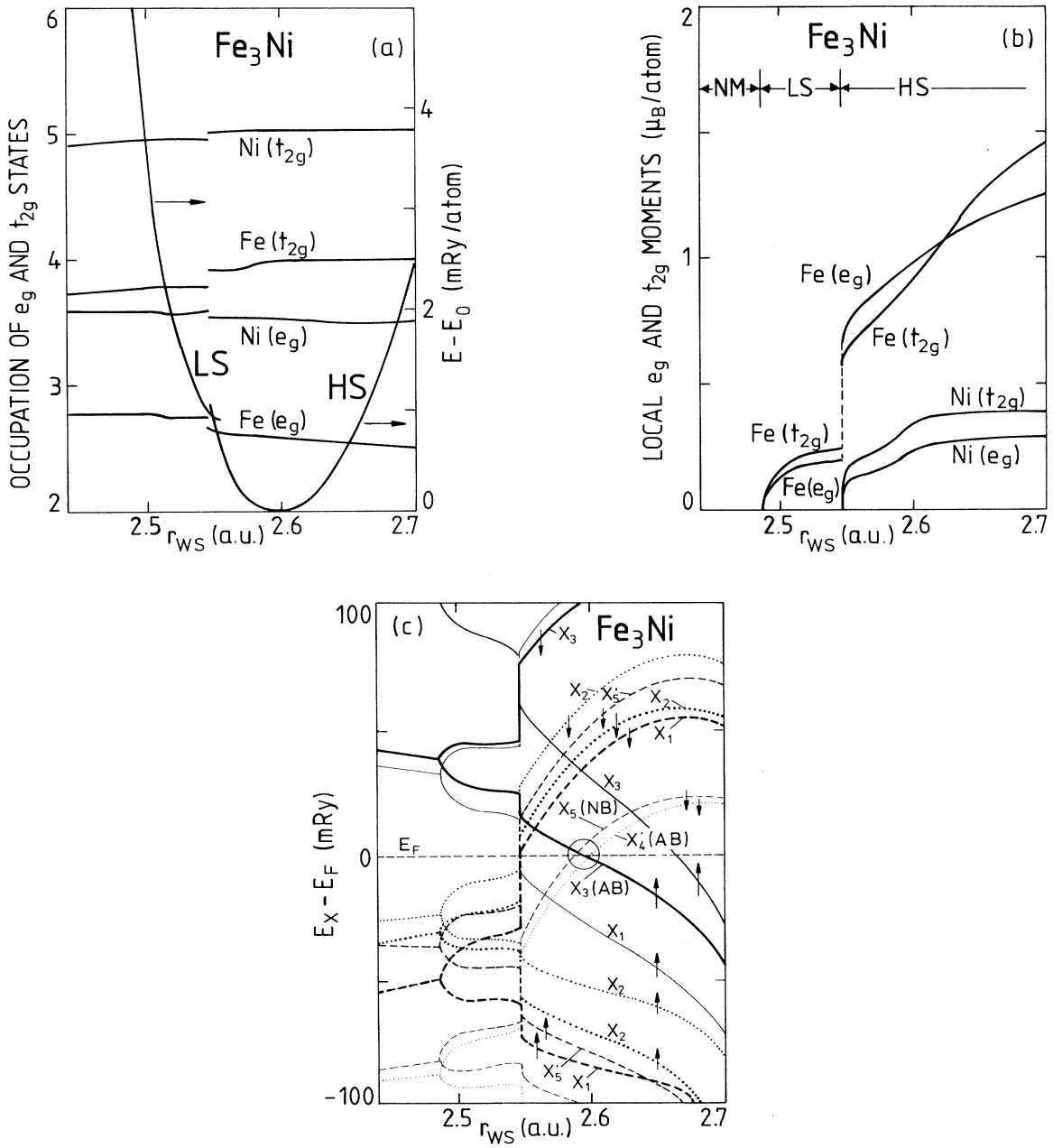

FIG. 2. (a) Volume dependence of the zero-field energy and e_g/t_{2g} state occupation (electrons) for Fe_3Ni; (b) volume dependence of the zero-field e_g and t_{2g} contributions to the local moment for Fe_3Ni; (c) volume dependence of e_g and t_{2g} eigenvalues (relative to E_F) at X for Fe_3Ni. Dotted curves correspond to e_g and solid and dashed curves to t_{2g} eigenvalues. Note the crossing of antibonding majority-spin (X_3), antibonding (X_4') and nonbonding (X_5) majority-spin states close to E_F (marked by a circle) in the ground state ($r_{WS}=2.60$ a.u.).

metry points and find that this kind of level crossing of states of different bonding character and spin symmetry is most pronounced for momentum vectors close to the X point.

Since results of early molecular-orbital-clusters calculations for Fe_{13}, $Fe_{12}Ni$, and Ni_{13} qualitatively agree with our considerations which are based on FSM calculations for Fe_3Ni, we briefly discuss the findings of Kaspar and Salahub. The cluster calculations showed that the physical basis of the phenomenological two-states model of Weiss is a rather peculiar situation at the Invar Fermi level where strongly antibonding majority-spin and nonbonding minority-spin orbitals lie close in energy, and that this situation exists only over a narrow range of Ni concentration. Kaspar and Salahub believe that emptying the antibonding majority-spin orbital with increasing temperature results in a contraction of the bonds which counteracts the vibrational lattice expansion. Our FSM calculations show that we indeed find this crossing of antibonding majority-spin and nonbonding minority-spin states at E_F on the HM site, while the same crossing occurs on the LM site at energies far below E_F. This is, in our opinion, one of the reasons why Invar can be typified by the HM state.

On the basis of this discussion we can conclude that if the Kaspar-Salahub explanation of the Invar effect is true, then it works only in the HM state. However, Kaspar and Salahub have not explained why, with increasing temperature and with decreasing exchange splitting, the same level crossing always occurs at E_F.

One possible mechanism which could stabilize and pin the observed level crossing close to E_F could be a strong coupling of electrons in the majority-spin AB X_3 and the minority-spin AB X_4' and NB X_5 states to those lattice modes which are responsible for the softening of the elastic constants. This would lead to a dynamic coupling and mixing of AB majority-spin and NB minority-spin states at elevated temperatures and could lead to a small gap in parts of momentum space which actually would pin the Fermi energy in the gap. This is investigated in the next section. Pinning of E_F would lead to small thermal expansion, since it hinders further charge transfer from e_g to t_{2g} states, which would be necessary to expand the lattice further.

Another possibility is that with decreasing exchange splitting this specific level crossing gets pinned very close to the magnetovolume instability. This then comes close to Moruzzi's picture, where the Invar effect is related to the observation that at high temperatures, the HM and LM states might merge. Hence the possibility of pinning E_F would explain why LM and HM states could remain lying close in energy over a large temperature range offering the possibility of a gradual transition from the HM ground state to a LM high-temperature state without any substantial change in volume.

We would like to remark that the crossing of states of different spin and bonding character at E_F occurs, of course, in most magnetic metals. Yet there is a remarkable difference with respect to level crossing and position of E_F in Invar and in stable magnets. This will be discussed in more detail in the next section. We also present results of a frozen phonon calculation which reveals the possibility of pseudogap formation due to kinetic effects.

III. THE ELECTRONIC STRUCTURE OF Fe_3Ni

All Invar-related features must have a microscopic origin. That means that a detailed study of the band structure and density of states is required. The spin-density-functional theory has shown that the total energy of a system is rigorously defined when the spin density is known. Practical application of this theory in the form of band-structure calculations using the local spin-density approximation for exchange and correlation[53,54] yields the well-established Stoner theory of itinerant magnetism. Our band-structure results are obtained from first-principles calculations employing the augmented spherical wave (ASW) method[55] which includes effects of exchange and correlation via the spin-density-functional theory. This treatment was extended by introducing the FSM method which allows the calculation of total energy as a function of the magnetic moment M and volume V, yielding an energy surface of the form $E(M,V)$ as is shown in Fig. 3 for the case of Fe_3Ni.

It has been shown that the total-energy surface contains the information needed to describe all macroscopic properties which are related to the Invar effect, as there is in particular, a very low critical pressure for the disappearance of magnetism and a large, negative magnetic contribution to the thermal expansion coefficient. Both features are related to a total-energy surface which is very flat in the M,V space. In this context, flat means that the difference in total energy between two extremal ($dE/dM=dE/dV=0$) points on the surface is small, being of the order of room temperature. It is evident that the existence of two separated magnetic states causing a magnetovolume instability is driven by the same mechanism which also causes a flat energy surface. That explains why most Invar systems are close to a magnetovolume instability although the existence of such an instability is no prerequisite for the existence of Invar-related phenomena.[43,45]

A. Density of states

Both iron and nickel are members of the $3d$ transition-metal series. As their atomic number differs only by 2, one expects that the electronic structure of alloys formed by these two elements shows a common band behavior. This means that the d bands of both constituents fully hybridize, showing most features of an fcc-like density of states. It must be noted that this common band behavior does not imply the applicability of a rigid-band picture. Such an oversimplification of an alloy system would imply an unphysical charge transfer from nickel to iron.[56] Because of the very similar electronegativity of both elements, such an *ionic* behavior does not occur. The different potentials for atomic number $Z=26$ and $Z=28$ and the different magnitude for the spin splitting cause different positions of the spin-up and spin-down d states at the two constituents. The hybridization between these

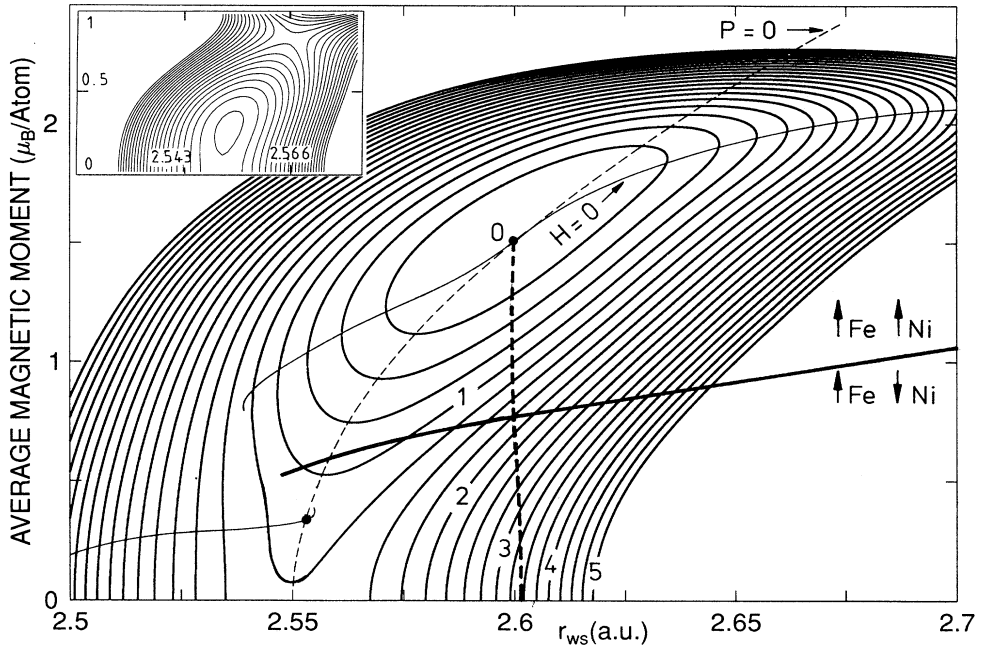

FIG. 3. Binding surface of Fe_3Ni obtained from FSM total-energy calculations. Energy contour lines are at 0.25 mRy/atom. Note that below the thick solid curve the Ni moment becomes unstable and orders antiparallel to the Fe moment. For larger values of the average magnetic moment per atom the Ni moment is forced to be parallel to the Fe moment. The dashed curve shows the temperature evoluiton of the system as obtained from the FSM-GL theory. The inset shows FSM-GL results for the LM state. Here, energy contour lines are at 0.02 mRy/atom.

states leads to a redistribution of the spectral weight of the density of states for Fe and Ni. This effect is known as covalent magnetism.[57]

This behavior is now investigated in detail. In the fcc structure each atom has 12 next neighbors. Experimentally, Fe_3Ni does not form an ordered structure; the atoms are randomly distributed on sites of an fcc lattice. In our investigation we approximate Fe_3Ni by the ordered Cu_3Au structure. Under this assumption each Fe atom is surrounded by 4 Ni and 8 Fe atoms, and each Ni atom has 12 Fe neighbors. One would therefore expect that the effect of covalent magnetism will be much stronger on Ni than on Fe. Analyzing the chemical bonds in terms of orbitals with e_g and t_{2g} symmetry, one finds that the e_g orbitals are always directed to atoms of the same kind, which are one lattice constant apart (compare Fig. 4). A bonding along such a large distance will always be weaker than one to next-nearest neighbors. Besides these Fe-Fe or Ni-Ni $dd\sigma$ bonds, there is the possibility for the $d_{x^2-y^2}$ orbitals to form a Fe-Ni $dd\pi$ bond

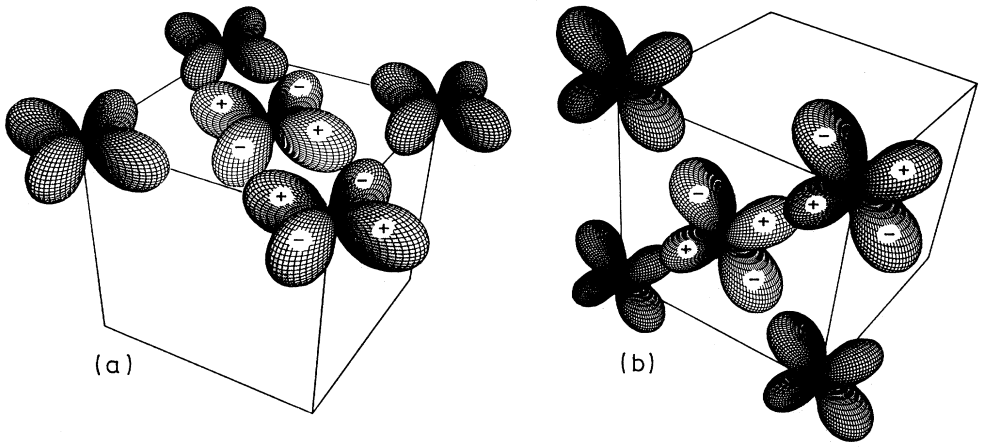

FIG. 4. (a) $dd\pi$ bonds of e_g orbitals and (b) $dd\sigma$ bonds of t_{2g} orbitals.

between two neighboring atoms. The t_{2g} orbitals point towards the 12 nn. This means that for a Ni atom all three t_{2g} orbitals form $dd\sigma$ bonds with Fe atoms. For an Fe atom, two of the three t_{2g} orbitals form Fe-Fe $dd\sigma$ bonds whereas the remaining t_{2g} orbital forms an Fe-Ni $dd\sigma$ bond. We therefore note that the Fe-Fe bonds will dominate the electronic structure of these types of alloys.

It is interesting to analyze the properties of the basic building block of the Fe_3Ni structure, which is given by an Fe atom together with its 12 neighbors forming the cluster $Fe[Fe_8Ni_4]$. For such a cluster the d states split, according to the ligand field model, into bonding and antibonding t_{2g} and t_{2g}^* states which, because of the strong $dd\sigma$ bond are well separated in energy and bonding, and antibonding e_g and e_g^* states which, because of the weaker $dd\sigma$ and $dd\pi$ bonds, lie between the t_{2g} states. Filling these states with the eight valence electrons of Fe leads to a cluster with a triplet ground state with the configuration $^3T_{1u}$ which is known to be unstable against a Jahn-Teller distortion.[58] Possible distortions can be tetragonal along the z axis, or a rotation of, e.g., the four Ni atoms against the remaining structure. Such ligand field considerations are not new and have specifically been used in the description of low-spin–high-spin transitions in Fe II complexes.[59–63]

It is noteworthy that the analogous cluster centered around a Ni atom (ten valence electrons) would be unstable, because all bonding and antibonding states are filled. For our analysis this means that any effects of the above kind should occur on the Fe sites. Although it is evident that in the metallic solid, the strong ligand fields which occur in an isolated cluster are reduced by the shielding effects of the conduction electrons, this simple model points in the right direction.

Highly precise band calculations for Fe_3Ni show the coexistence of the LM and the HM states in a limited volume range around a Wigner-Seitz radius of $2.55\mu_B$/atom [see Figs. 2(a) and 3]. In Fig. 5 we show the Fe/Ni decomposed densities of states for the LM [5(a)] and the HM [5(b)] solutions, respectively. In addition, Figs. 6(a) and 6(b) display the Γ to X bands and the local densities of states for the majority and minority HM states decomposed into e_g and t_{2g} contributions.

In the LM case the magnetic moment appears almost exclusively on the iron atoms. The reason for this behavior is that the Fermi energy lies in a region of very low DOS for Ni and high DOS for Fe. The DOS of the d electrons of Fe in the nonmagnetic state is high enough to fulfill the Stoner criterion. Thus Fe becomes unstable against a spontaneous band splitting. In the LM case, the band splitting is small so that effects of covalent magnetism are also very small. We find the bands almost rigidly shifted, causing the magnetic moment to be zero on Ni and finite on Fe only. The vanishing moment on the Ni site is not only a consequence of the low DOS; the small moment of the d electrons is compensated by the antiparallel moments of the s and p electrons. In the LM state, the Fermi energy for both spin directions lies in a minimum of the e_g DOS of iron (not shown), a position which leads to the local total-energy minimum for the LM state. For the HM solution [Figs. 6(a)–6(f)] the situation is changed. Although a rigid-band model is no longer valid, Figs. 5(a) and 5(b) show how the Fermi energy moves while going from the LM to the HM state. In the majority band the Fermi energy passes through a high peak in the DOS. This peak causes an energy bar-

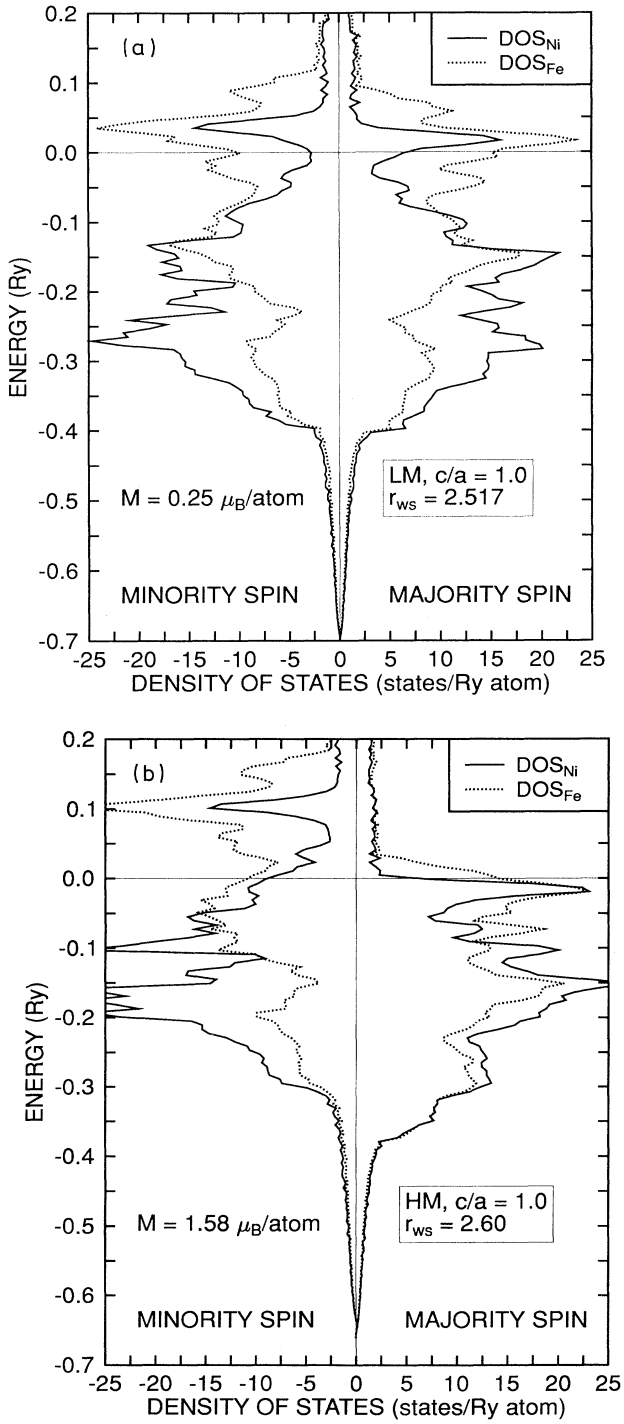

FIG. 5. Iron and nickel densities of states of (a) the low-moment and (b) the high-moment states.

rier between the LM and HM states. The system Fe-Ni is thus an example of a metamagnet.

Figure 2(b) shows how this metamagnetic behavior evolves with increasing volume. For small volumes the system is in a nonmagnetic state. At a Wigner-Seitz radius of $r_{WS}=2.475$ a.u., the LM state starts and is found as a single minimum in the total energy vs magnetic moment (M) curve. The HM state appears at $r_{WS}=2.545$ a.u., being at first metastable with respect to the LM state. In the volume range from $r_{WS}=2.545-2.555$ a.u., we find a coexistence of both the LM and HM states. The $E(V)$ curve describing this two-phase region has two minima at the respective magnetic moments. For $r_{WS}>2.555$ a.u., the LM state disappears and only the HM solution remains.

B. The high-moment state

The equilibrium volume is found at about $r_{WS}=2.6$ a.u. where only the HM state exists. The splitting of the nickel bands is limited by the small number of holes in the nickel d band, leading to a full majority band and a magnetic moment of about $0.6\mu_B$ per nickel atom [Fig. 2(b)] as in pure fcc Ni. The magnetic moment at the iron site is found to be about $1.9\mu_B$ per iron atom. This value is not only smaller than that of bcc Fe ($2.2\mu_B$), but also is smaller than the value one would expect for a hypothetical fcc Fe ($2.6\mu_B$). This effect is due to the different degree of hybridization between the majority-spin bands which are about equal in energy and the minority bands of nickel and iron which lie at different energies. This energy difference is not only caused by the different band splitting, but also by the fact that a charge transfer from nickel to iron is avoided by the more repulsive potential of the almost full Ni d band pushing the Fe states even higher up on the common energy scale. This effect leads to what is known as covalent magnetism. The combination of all these effects causes the Fermi energy to take on a special position in the band structure. For majority spin, E_F lies in a region of antibonding states of mainly t_{2g} character with a small admixture of states with e_g symmetry. For minority spin, E_F is found in the nonbonding states which are composed of about equal amounts of states of both symmetry directions. The high DOS at the iron site compensates for the *strongly* magnetic behavior of Ni and leads to the high susceptibility observed. This positioning of E_F between antibonding and nonbonding states resembles the findings of Kaspar and Salahub.

C. Band structure and tetragonal distortion

The band structure of the cubic Fe_3Ni phase is shown in Fig. 6. We have chosen bands along the Δ symmetry line between the center of the Brillouin zone (BZ) labeled Γ and the point X on the surface of the first BZ. In the LM case there is only a minor change in the band structure compared to the nonmagnetic state. The pronounced t_{2g} peak for Ni, just above the Fermi energy is shown in the band structure by the flat Δ_2' band starting from Γ, whereas the Δ_5 band is of mainly Fe t_{2g} character.

The larger energy separation of this Δ_2' band leads to the region of very low DOS at the top of the Ni d band. Even for the small splitting in the LM state, a broadening of the minority bands is found, which is due to the different energies for the Fe and Ni states. The HM case (Fig. 6) finds the Fermi energy in a very special position. For majority spin, we find a flat band of Δ_2' character which consists mainly of antibonding Ni t_{2g} states. This band is responsible for the sharp peak in the Ni majority t_{2g} DOS next to the Fermi energy. The antibonding t_{2g} and e_g states at the top of the Fe d band stem from the Δ_1 and Δ_5 bands crossing the Fermi energy, respectively. For minority spin, the Fermi energy is found at a crossing of nonbonding bands of Δ_1 and Δ_5 character. From the DOS (Fig. 6) one notices that the Fermi energy is exactly at a crossover region where the Fe DOS changes from mainly t_{2g} to mainly e_g symmetry. In the total DOS this leads to a valley which is sufficient to stabilize the magnetic moment. This analysis now resembles the findings of Kaspar and Salahub who, from a molecular-orbital cluster calculation, stated that for the Invar alloys there is a *rather peculiar situation* at the Invar Fermi level where strongly antibonding majority-spin orbitals and nonbonding minority-spin orbitals lie closely together. This is exactly the situation we find from the present band-structure calculation. A very similar analysis was given by Johnson *et al.*,[12] who calculated the self-consistent electronic structure of disordered Fe-Ni using the KKR-CPA formalism.

To study the stability against a tetragonal distortion along the z axis we performed a set of band-structure calculations where we changed the c/a ratio from 1 (cubic case) to values between 0.95 and 1.075. Figure 7 shows the results for the majority-spin and minority-spin bands and for the individual DOS for the isochore tetragonal distortion with $c/a=1.075$. From the ligand field model one expects that the Γ_{12} (e_g) states split symmetrically into Γ_1^+ and Γ_3^+ and the $\Gamma_{25}'(t_{2g})$ splits asymmetrically into a two-dimensional Γ_5^+ and a one-dimensional Γ_4^+. Comparing the majority-spin band structures for the $c/a=1$ (cubic) [Fig. 6(a)] and the $c/a=1.075$ (tetragonal) [Fig. 7(a)] cases, one notices that, apart from the lifted degeneracies and a few avoided crossings, the flat Δ_2' band is pushed down in energy away from E_F. This leads to a pronounced dip in the majority-spin DOS at the Fermi energy.

The change in the minority-spin bands is also interesting. For the cubic case we find a crossing of a Δ_1 and a Δ_5 band close to the X point [Fig. 6(d)]. For the tetragonal distortion, these bands no longer cross but open a gap exactly at the Fermi energy [Fig. 7(b)]. The opening of a gap is also seen in the minority-spin DOS curves where a gap (valley) in the e_g DOS of Fe atoms is found near E_F. This gap has an additional pinning effect on the Fermi energy, and explains why the magnetic moment remains constant over the range of distortions investigated. It must be noted that this noncrossing of the bands is not due to symmetry but to the energetics of the system. A

change of the c/a ratio leads to a change of the overlap of certain orbitals and subsequently to a change in the dispersion of the respective bands. Although this effect is not the same as the original Jahn-Teller effect, where the breaking of the symmetry is responsible for the instability against a distortion, the consequences which can be drawn from the lowering of the band energy are equivalent. To some extent the effect described in this

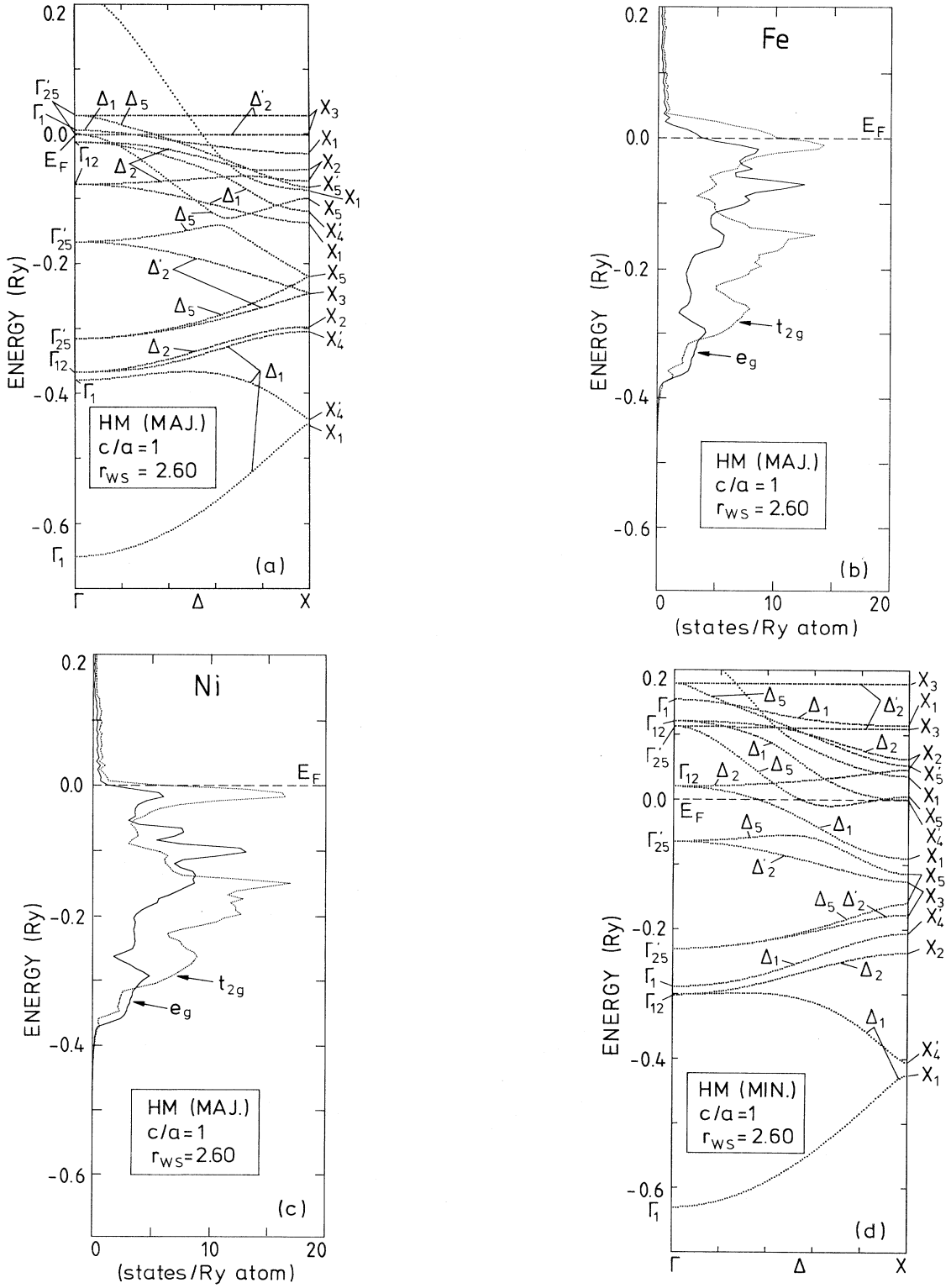

FIG. 6. Band structure along the Γ-X direction, e_g and t_{2g} decomposed densities of states of iron and nickel for (a–c) majority spin and (d–f) minority spin.

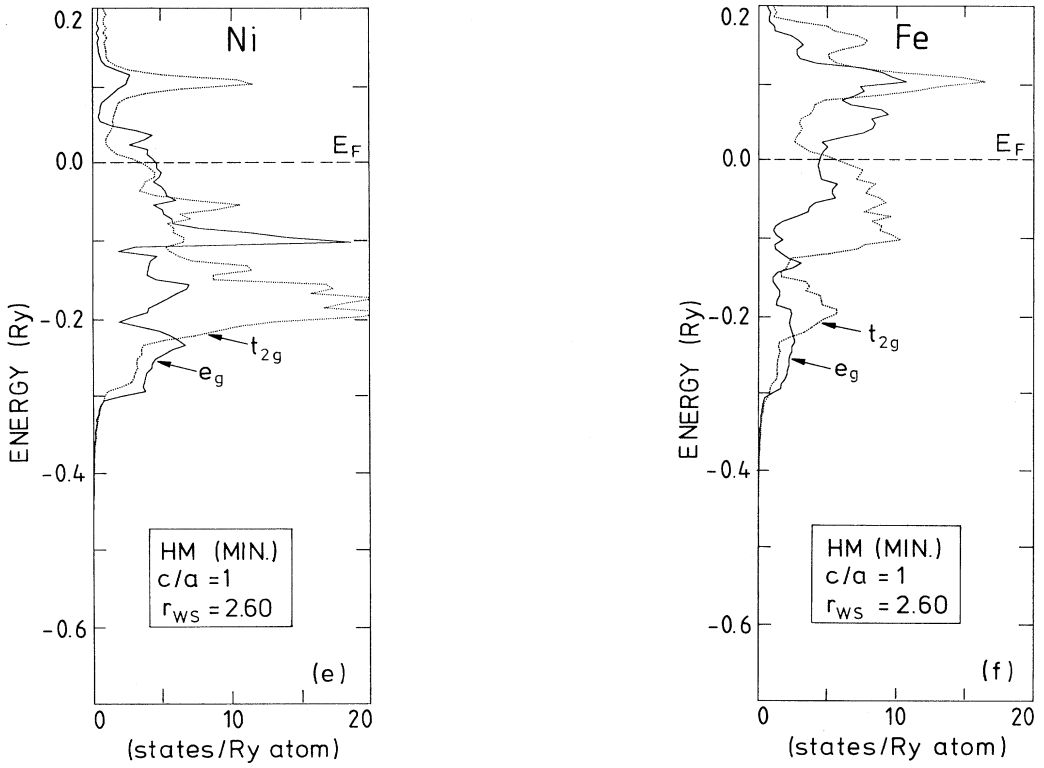

FIG. 6. (*Continued*).

paper is the solid-state analog to the Jahn-Teller instability of the $Fe[Fe_8Ni_4]$ cluster discussed in Sec. III A.

The phase diagram of $Fe_{1-x}Ni_x$ (Fig. 1) shows a martensitic transition from the γ phase (fcc) to the α phase (bcc) very close to the actual Invar region. According to Bain[64] this transition can be mimicked by a tetragonal distortion, where the c/a ratio changes from $\sqrt{2}$ to 1, for the fcc lattice assumed as a tetragonal body-centered lattice with dimension $(a,a,a\sqrt{2})$ and the bcc lattice with dimension (a',a',a'), respectively (if a_0 is the original fcc lattice constant, then $a=a_0\sqrt{2}/2$).

Because of the band splitting due to such a distortion, this mechanism is energetically favored, so that e.g., a thermally induced tetragonal phonon mode can give rise to the onset of the Bain transition. It is not purely coincidential that the bands which are responsible for the In-

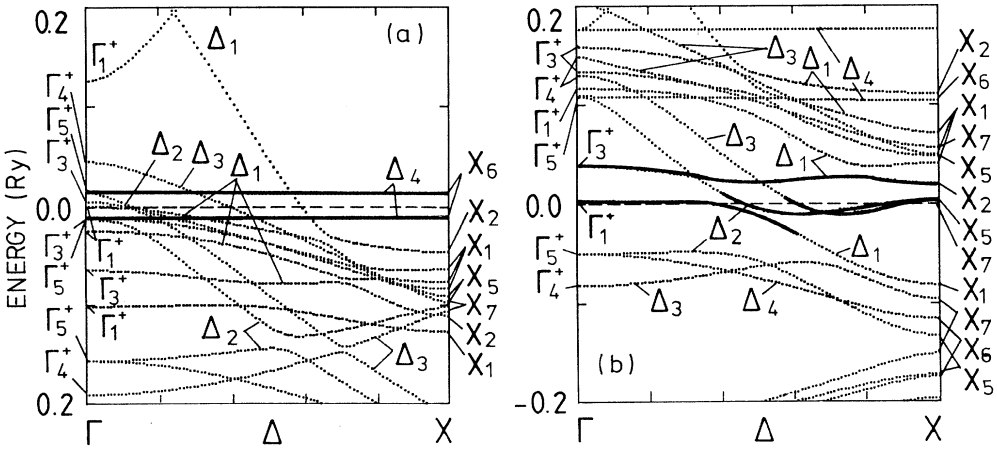

FIG. 7. (a) Majority-spin and (b) minority-spin band structure along the Γ-X direction for the case of an isochore tetragonal distortion in Fe_3Ni ($c/a=1.075$, $r_{WS}=2.60$). The thick solid curves indicate where a pseudogap opens close to E_F which leads in the DOS to a pronounced dip.

var effect are also responsible for the instability against a tetragonal distortion. This would explain why the Invar effect usually occurs close to a martensitic phase transition.[23] Figure 8 shows results for the total energy and the magnetic moment when we follow Bain's path from the fcc to the bcc structure. These calculations are done by using the constraint that the nn Fe-Fe distance does not change during the transformation (in this case the bcc lattice constant is given by $a'=a_0\sqrt{2/3}$). Although ASW total energies of tetragonal distorted lattices can be in error because of the atomic shear approximation, our results for the lattice constant and the magnetic moment of the bcc structure compare well with experiment.

Both the Invar effect and the martensitic phase transition require the Fermi energy to lie at a very special position in the band structure. It has been found experimentally that, independently of the alloy system, the Invar effect always occurs around an average valence electron number of 8.6e/atom. This *magic number* might be understood from the fact that most of the Invar systems are alloys of transition-metals atoms whose atomic number does not differ very much. These alloys usually show the common band behavior described in Sec. III A, which makes it clear that the critical feature in the band structure always appears at the same position. For a transition metal, one usually finds only 0.6 sp electrons/spin because the remaining 0.4 electrons are transferred into the d band via the $s-d$ hybridization.[65] In the HM state the majority-spin band is almost filled and on the average contains 4.5 d electrons. The remaining 2.9 electrons occupy the majority-spin band and fill those states exactly to the band crossing described above. This distribution of majority- and minority-spin electrons also explains why most of the Invar systems show an average magnetic moment of about $1.6\mu_B$/atom. Increasing or decreasing the e/atom ratio sets the Fermi energy above or below the band crossing so that the described effects can no longer occur.

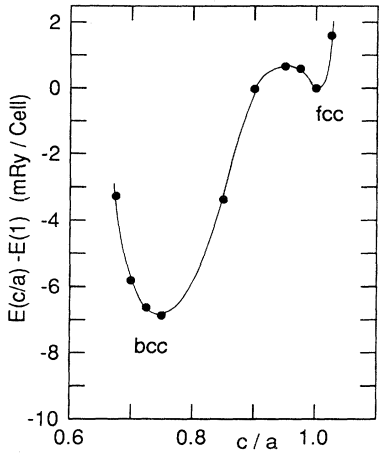

FIG. 8. Results of total-energy calculations for Fe_3Ni for the Bain transformation from the fcc to the bcc structure. The energy difference between the two structures is of the order of 1.5 mRy/atom. Note that the volume of the bcc structure is larger than the fcc structure. This is achieved by keeping the distance between neighboring Fe atoms constant during the transformation. Fcc: $r_{WS}=2.60$ a.u., $M=1.56\mu_B$/atom. Bcc: $r_{WS}=2.67$ a.u., $M=2.11\mu_B$/atom.

IV. FSM-GL DESCRIPTION OF THE MAGNETOVOLUME INSTABILITY IN Fe_3Ni

The FSM-GL theory has been used to describe itinerant magnetism in a series of transition-metal alloys. In the case of coexisting LM and HM states near a magnetovolume instability as in Fe_3Ni, the FSM-GL theory used so far must be modified in order to account for the two different ground states.

If one compares the binding surface of Fe_3Ni (Fig. 3) with the binding surfaces of the constituents, one gets the impression that the surface of Fe_3Ni is a superposition of the fcc Fe[66] and Ni[45] surfaces. With respect to magnetic moment and volume, the LM and the HM states of Fe_3Ni correspond to the LM state of fcc Ni and the HM state of fcc Fe, respectively. However, we have shown in the preceding section that in Fe_3Ni the Ni moment cannot be stabilized in the LM state, which is at the borderline where the Ni moment starts to order antiferromagnetically (Fig. 3).

An FSM-GL expansion in terms of the average magnetic moment and elastic contributions is not susceptible enough to account for this antiferromagnetic ordering. Therefore, if we think that the GL expansion corresponds to the continuum limit of an effective localized spin model for Fe_3Ni, we should use an expansion in terms of two magnetization fields, one for Fe and one for Ni. In addition we must add a constraint which fixes the average magnetic moment per atom. This leads to

$$\mathcal{H}=\frac{1}{V}\int d^3r\left[\frac{1}{2}B\omega^2+\gamma\omega^3+\delta\omega^4+a_1(\omega_1-\omega)\mathbf{m}_1^2(\mathbf{r})+b_1\mathbf{m}_1^4(\mathbf{r})+c_1\mathbf{m}_1^6(\mathbf{r})+d_1\mathbf{m}_1^8(\mathbf{r})+a_2(\omega_2-\omega)\mathbf{m}_2^2(\mathbf{r})\right.$$
$$\left.+b_2\mathbf{m}_2^4(\mathbf{r})+c_2\mathbf{m}_2^6(\mathbf{r})+d_2\mathbf{m}_2^8(\mathbf{r})+J_1\mathbf{m}_1^2(\mathbf{r})\mathbf{m}_2^2(\mathbf{r})+J_2\mathbf{m}_1(\mathbf{r})\mathbf{m}_2^3(\mathbf{r})+J_3\mathbf{m}_1^3(\mathbf{r})\mathbf{m}_2(\mathbf{r})\right], \quad (1)$$

$$\mathbf{M}(\mathbf{r})=\tfrac{1}{4}[3\mathbf{m}_1(\mathbf{r})+\mathbf{m}_2(\mathbf{r})]\ . \quad (2)$$

Here, m_1 is the Fe and m_2 the Ni moment; $\omega=(V(T)-V_0)/V_0$ is the relative volume, V_0 a reference volume, B the bulk modulus, and $\omega_{1,2}$ are introduced for convenience.

Calculations are done according to the FSM method. We fix the average magnetic moment per atom and determine the individual moments self-consistently. This leads to a binding surface with coexisting LM and HM states

close to the instability. GL parameters are obtained from a fit to the original FSM binding surface (Fig. 3). This fit shows that the binding surface can indeed be considered as a superposition of an Fe and Ni surface. In the calculation we allow the Ni moment to be antiparallel to the Fe moment. This arrangement is indeed stable at low values for the average moment. At larger average moment values, the Ni moment is forced to be parallel to the Fe moment. Thus, this theory reproduces the results of the FSM total-energy calculations. The inset in Fig. 3 shows the fine structure around the LM state obtained with the FSM-GL theory. It closely resembles the fine structure of Fe_3Pt which Podgórny has obtained in his FSM-LMTO calculation.[67]

With increasing temperature we expect that the LM and the HM states come closer and finally merge at T_c. We would like to stress that for a GL expansion using a single magnetization field, HM and LM states do not merge with increasing T. They are independent ground states. In the extended FSM-GL theory used here, it is the constraint for the average moment which can force the HM and the LM states to merge. We consider this as a typical Invar effect, since the merging of high-volume and low-volume states means low thermal expansion. However, this is not the basic mechanism for Invar behavior, since the discussion in the preceding section has shown that Invar is associated with a subtle charge transfer concerning electrons in states close to E_F. Nevertheless, the merging of the HM and LM states can be considered as an important aspect of Invar.

For true Invar composition, $Fe_{65}Ni_{35}$, statistical disorder of the atoms on the fcc lattice will lead to more than two states because of local environment effects. First results of supercell calculations for Fe_5Ni_3 show that it is not the Ni moment which is unstable in Invar but one of the Fe moments is unstable in an otherwise ferromagnetic matrix. This comes close to experimental findings.[68,69] The stability of the Fe moment and the instability of the Ni moment in Fe_3Ni show that this compound is not a true Invar system.

In spite of its success the FSM-GL theory has the disadvantage that it cannot describe microscopically the competition of bonding, magnetism, and structural stability. To do this a microscopic theory is needed. Since this is beyond the scope of the present paper, we only outline in which frame the electronic details addressed in Sec. III can be discussed. A good starting point is the multiband Hubbard model for s,p, and d electrons with simple coupling to the volume,

$$\mathcal{H}_0=\sum_{n\mathbf{k}\sigma}[\varepsilon^0_{n\mathbf{k}\sigma}+(\partial\varepsilon^0_{n\mathbf{k}\sigma}/\partial\omega)_0\omega]\times a^\dagger_{n\mathbf{k}\sigma}a_{n\mathbf{k}\sigma}+\tfrac{1}{2}B\omega^2+\gamma\omega^3+\delta\omega^4\ , \tag{3}$$

$$\mathcal{H}_1=\frac{1}{2}\sum_{i\sigma\sigma'}\sum_{\alpha\beta\gamma\delta}U_{\alpha\beta\gamma\delta}a^\dagger_{i\alpha\sigma}a^\dagger_{i\beta\sigma'}a_{i\gamma\sigma'}a_{i\delta\sigma}\ , \tag{4}$$

where $a^{(\dagger)}_{i\alpha\sigma}$ is the creation (destruction) operator of an electron at the lattice site $\mathbf{R}_i$ in orbital α with spin σ, and ω is as before, the relative volume. Note that the Bloch energies are given by $\varepsilon^0_{n\mathbf{k}\sigma}$ plus the one-electron contributions from $\mathcal{H}_1$, whereby expectation values must be evaluated self-consistently. $\mathcal{H}_1$ contains only local Coulomb correlation and exchange terms.

A good fit to the FSM band structure of Fe_3Ni is obtained if we keep a single intraatomic Coulomb integral U (for electrons in the same d orbital) and U' (for electrons in different d orbitals) and a single intraatomic exchange integral J for the d electrons. The renormalization of the single-particle energies $\varepsilon^0_{n\mathbf{k}\sigma}$ due to the interaction terms we have kept is obvious from a Hartree-Fock decomposition of $\mathcal{H}_1$, which leads to

$$\mathcal{H}_1=-\frac{U}{2}\sum_{i,\mu}\langle\boldsymbol{\sigma}_{i\mu}\rangle\boldsymbol{\sigma}_{i\mu}+\sum_i\left[\left[U'-\frac{J}{2}\right]\langle n_i\rangle n_i+\sum_\mu\left[\frac{U}{2}+J-U'\right]\langle n_{i\mu}\rangle n_{i\mu}\right]$$
$$+\sum_{i,\mu\neq\mu',\sigma}[(U'-J)\langle a^\dagger_{i\mu\sigma}a_{i\mu'\sigma}\rangle a^\dagger_{i\mu'\sigma}a_{i\mu\sigma}+J\langle a^\dagger_{i\mu-\sigma}a_{i\mu'-\sigma}\rangle a^\dagger_{i\mu'\sigma}a_{i\mu\sigma}-U'\langle a^\dagger_{i\mu\sigma}a_{i\mu'-\sigma}\rangle a^\dagger_{i\mu'-\sigma}a_{i\mu\sigma}]\ . \tag{5}$$

Here, $\boldsymbol{\sigma}_{i\mu}=(2/\hbar)\mathbf{S}_{i\mu}$ is the spin operator of the d electrons in orbital μ, $\langle n_{i\mu}\rangle$ is the number of d electrons in orbital μ, and $\langle n_i\rangle$ is the total number of d electrons. The terms in the second line of (5) are local charge-transfer terms, whereas the last term contains an anomalous expectation value which mixes states of different bonding and spin character. The self-consistent evaluation of this term will help to describe the electronic structure of Fe_3Ni along the lines discussed in Sec. III. This term leads to a pseudogap in the electronic spectrum which vanishes at T_c. It also may serve to describe the crossover from the HM to the LM state with increasing T. Therefore, we may consider this anomalous expectation value as the *order parameter of Invar*. Due to the presence of the volume terms in (3), the charge-transfer terms and the order parameter will strongly depend on the volume. This brief discussion of (4) and (5) shows that this Hamiltonian is useful for first-principle FSM calculations at finite temperatures.[70]

V. CONCLUSIONS

In the present work we elucidated some of the microscopic mechanisms which seem to be responsible for the Invar effect and the related instability against a martensitic phase transition. The central feature of our findings is that the Fermi energy is found in a very special position in the minority-spin band. Our first-principles band calculations confirmed the earlier result by Kaspar and Salahub drawn from cluster investigations. We find that for majority spin, E_F lies in a high peak of e_g and t_{2g} an-

tibonding states. In the minority band, E_F is found between t_{2g} nonbonding and e_g antibonding states. In terms of a single-particle picture the following mechanism should take place: on thermal excitation, electrons can be transferred from majority-spin antibonding states to minority-spin nonbonding states. Because of the large number of states for both spin directions around E_F this mechanism should occur at low enough temperatures, and should also explain the observed rapid drop in the magnetic moment for low temperatures. Unfortunately, the characteristic temperatures which scale the single-particle excitations are of the order of 2000–6000 K for the transition metals[71] so that single-particle excitations cannot be responsible for the Invar effect. The position of the Fermi energy in the minority band, being at the crossover between nonbonding and antibonding states, is also responsible for the tendency of most Invar systems to undergo a martensitic phase transition.

Thus we have two competing energies in the system: one is related to the energy gain in Fe_3Ni upon structural changes from the fcc to the bcc structure; the other is related with the magnetovolume instability and corresponds to the energy difference of the HM and LM states. The lower one of these *excitation* energies will determine whether, at a given concentration of Ni atoms, Invar with premartensite or martensite is the stable low-temperature phase.

In Fig. 7 we have shown the opening of the gap due a static tetragonal distortion simulating a phonon of the desired symmetry. This gap between the nonbonding and antibonding states results in two effects. First, the gain in nonbonding states and the loss in antibonding states lead to a shrinking of the lattice as desired for an Invar behavior. Second, because of the gain in band energy due to the formation of the gap, this mechanism favors a possible martensitic change to the bcc structure along this Bain transition path. We also expect that the gap actually can pin the Fermi energy which could explain the low thermal expansion in Invar alloys over a large temperature range.

ACKNOWLEDGMENTS

One of us (P.E.) wishes to acknowledge stimulating discussions with Professor Wassermann, Professor Acet, Dr. Dumpich, Professor Reinen, and Professor Gütlich. This work has been supported by the Deutsche Forschungsgemeinschaft in the frame of the Sonderforschungsbereich 166.

[1]C. E. Guillaume, C. R. Acad. Sci. **125**, 235 (1897).
[2]E. F. Wassermann, in *Ferromagnetic Materials*, edited by K. H. J. Buschow and E. P. Wohlfarth (North-Holland, Amsterdam, 1990), Vol. 5, p. 237.
[3]R. J. Weiss, Proc. R. Soc. London **82**, 281 (1963).
[4]Y. Kakehashi, Physica B **161**, 143 (1989).
[5]Y. Kakehashi, Prog. Theor. Phys. Suppl. **101**, 105 (1990).
[6]Y. Kakehashi, J. Phys. Soc. Jpn. **49**, 2124 (1980).
[7]H. Hasegawa, J. Phys. C **14**, 2793 (1981).
[8]H. Hasegawa, J. Phys. Soc. Jpn. **51**, 767 (1982).
[9]A. R. Williams, V. L. Moruzzi, C. D. Gelatt, Jr., J. Kübler, and K. Schwarz, J. Appl. Phys. **53**, 2019 (1982).
[10]V. L. Moruzzi, Phys. Rev. B **41**, 6939 (1990).
[11]V. L. Moruzzi, Solid State Commun. **83**, 739 (1992).
[12]D. D. Johnson, F. J. Pinski, and G. M. Stocks, J. Appl. Phys. **57**, 3018 (1985).
[13]D. D. Johnson, F. J. Pinski, and J. B. Staunton, J. Appl. Phys. **61**, 3715 (1987).
[14]D. D. Johnson, F. J. Pinski, J. B. Staunton, B. L. Györffy, and G. M. Stocks (unpublished).
[15]S. Krompiewski, U. Krauss, and U. Krey, Phys. Rev. B **39**, 2819 (1989).
[16]S. Krompiewski, U. Krey, and H. Ostermeier, J. Magn. Magn. Mater. **69**, 117 (1987).
[17]S. Krompiewski, U. Krey, U. Krauss, and H. Ostermeier, J. Magn. Magn. Mater. **73**, 5 (1988).
[18]H. Früchtel and U. Krey, J. Magn. Magn. Mater. **94**, L20 (1991).
[19]E. I. Kondorsky and V. L. Sedov, J. Appl. Phys. **31**, 331 (1960).
[20]J. B. Müller and J. Hesse, Z. Phys. B **54**, 35 and 43 (1983).
[21]R. Kloss, Int. J. Magn. **5**, 251 (1973).
[22]E. F. Wassermann, M. Acet, and W. Pepperhoff, J. Magn. Magn. Mater. **90&91**, 1260 (1990).
[23]E. F. Wassermann, J. Magn. Magn. Mater. **100**, 346 (1991).
[24]V. L. Moruzzi, Physica B **161**, 99 (1989).
[25]V. L. Moruzzi, P. M. Marcus, and J. Kübler, Phys. Rev. B **39**, 6957 (1989).
[26]M. Podgórny, Physica B **161**, 105 (1989).
[27]G. L. Krasko, Phys. Rev. B **36**, 8565 (1987).
[28]M. M. Abd-Elmeguid and H. Micklitz, Physica B **161**, 17 (1989).
[29]J. Kaspar and D. R. Salahub, Phys. Rev. Lett. **47**, 54 (1981).
[30]M. Podgórny, Acta Phys. Pol. A **78**, 941 (1990).
[31]E. P. Wohlfarth, Physica B&C **91**, 305 (1977).
[32]T. Moriya and K. Usami, Solid State Commun. **34**, 95 (1980).
[33]E. P. Wohlfarth, Solid State Commun. **35**, 797 (1980).
[34]M. Shimizu, J. Magn. Magn. Mater. **10**, 231 (1979).
[35]M. Shiga, Prog. Theor. Phys. Suppl. **101**, 475 (1990).
[36]K. K. Murata and S. Doniach, Phys. Rev. Lett. **29**, 285 (1972).
[37]Takahashi, J. Phys. Condens. Matter **2**, 8405 (1990).
[38]A. R. Williams, V. L. Moruzzi, J. Kübler, and K. Schwarz, Bull. Am. Phys. Soc. **29**, 278 (1984).
[39]K. Schwarz and P. Mohn, J. Phys. F **14**, L129 (1984).
[40]P. Entel and M. Schröter, J. Phys. (Paris) Colloq. **8**, 293 (1988).
[41]P. Entel and M. Schröter, Physica B **161**, 121 (1989).
[42]D. Wagner, J. Phys. Condens. Matter **1**, 4635 (1989).
[43]M. Schröter, P. Entel, and S. G. Mishra, J. Magn. Magn. Mater. **87**, 163 (1990).
[44]M. Schröter and P. Entel, Physica B **165&166**, 229 (1990).
[45]P. Mohn, K. Schwarz, and D. Wagner, Phys. Rev. B **43**, 3318 (1991).
[46]P. Entel, M. Schröter, J. Zielinski, and S. G. Mishra, in *Electronic Correlation and Disorder in Metals*, edited by S. N. Behera (World Scientific, Singapore, 1991), p. 345.
[47]P. Entel, in *Strongly Correlated Electron Systems and High-T_c Superconductivity*, edited by E. Zipper, R. Mańka, and M. Maśka (World Scientific, Singapore, 1991), p. 38.
[48]M. Schröter, B. Schmitz, and P. Entel, J. Magn. Magn. Mater.

104-107, 747 (1992).
[49]M. Schröter and P. Entel (unpublished).
[50]M. Shiga, K. Makita, K. Uematsu, Y. Muraoka, and Y. Nakamura, J. Phys. Condens. Matter **2**, 1239 (1990).
[51]Ll. Mañosa, G. A. Saunders, H. Rahdi, U. Kawald, J. Pelzl, and H. Bach, Phys. Rev. B **45**, 2224 (1992).
[52]C. S. Wang, B. M. Klein, and H. Krakauer, Phys. Rev. Lett. **54**, 1852 (1985).
[53]U. von Barth and L. Hedin, J. Phys. C **5**, 1629 (1972).
[54]J. F. Janak, Solid State Commun. **25**, 53 (1978).
[55]A. R. Williams, J. Kübler, and C. D. Gelatt, Jr., Phys. Rev. B **19**, 6094 (1979).
[56]K. Schwarz, P. Mohn, P. Blaha, and J. Kübler, J. Phys. F **14**, 2659 (1984).
[57]A. R. Williams, R. Zeller, V. L. Moruzzi, C. D. Gelatt Jr., and J. Kübler, J. Appl. Phys. **52**, 2067 (1981).
[58]D. Reinen and M. Atanasov, Magn. Reson. Rev. **15**, 167 (1991).
[59]It should be noted that the denomination low-moment–high-moment state should be preferred to low spin–high spin, because the latter refers to the magnetic state of chemical complexes, a picture in terms of localized spins which must not be mixed up with itinerant moments found in our metallic system. Note, that Fe II complexes are insulators and that due to the large distance between the Fe ions there is no exchange field which mediates the magnetic state. Instead it is the strength of the ligand field which determines whether the individual Fe ion is in the LS or HS state. Therefore, we distinguish the LS, HS states in Fe II complexes from the LM, HM states in metals. The simultaneous transition of many Fe ions from the LS ground state to the HS state, which occurs in Fe II complexes at elevated temperatures, is caused by the cooperative Jahn-Teller effect.
[60]P. Gütlich, in *Structure and Bonding,* edited by M. J. Clarke, J. B. Goodenough, P. Hemmerich, J. A. Ibers, C. J. Jorgensen, J. B. Neilands, D. Reinen, R. Weiss, and R. J. P. Williams (Springer, Berlin, 1981), Vol. 44, p. 83.
[61]D. Reinen, A. Ozarowski, B. Jacob, J. Pebler, H. Stratemeier, K. Wieghardt, and I. Tolksdorf, Inorg. Chem. **26**, 4010 (1987).
[62]N. Willenbacher and H. Spiering, J. Phys. C **21**, 1423 (1988).
[63]H. Spiering and N. Willenbacher, J. Phys. Condens. Mater. **1**, 10089 (1989).
[64]E. C. Bain, Trans. AIME **70**, 25 (1924).
[65]A. P. Malozemoff, A. R. Williams, V. L. Moruzzi, and K. Terakura, Phys. Rev. B **30**, 6565 (1984).
[66]V. L. Moruzzi, P. M. Marcus, K. Schwarz, and P. Mohn, Phys. Rev. B **34**, 1784 (1986).
[67]M. Podgórny (unpublished).
[68]H. Zähres, M. Acet, W. Stamm, and E. F. Wassermann, J. Magn. Magn. Mater. **72**, 80 (1988).
[69]A. Z. Men'shikov, A. E. Teplykh, and V. L. Kuznetsov (unpublished).
[70]P. Entel (unpublished).
[71]O. Gunnarsson, J. Phys. F **6**, 587 (1976).